polyhedron geometry[18] is similar to that of Co(terpy)$(NCO)_2$, in the other the polyhedron is approximately a square pyramid.[19] This finding may explain that Cu(terpy)Cl_2—in contrast to the thiocyanate and the bromide complexes—has a different geometry, namely a strongly elongated square pyramid.[4,5] We have also measured the EPR spectra of the two complexes (130 K) in frozen DMF and DMSO solutions but did not succeed in obtaining signals in more nonpolar solvents for solubility reasons. Surprisingly, completely different **g** tensors from those in the solid state were obtained. They are tetragonal within the line width for the thiocyanate (Figure 6) and only slightly orthorhombic for the bromide. Both spectra are strongly indicative of (approximately) square-pyramidal geometries [$g_\parallel = 2.25_6$ (2.26_5), $g_\perp = 2.06_4$ ($\simeq 2.05$) for $x = NCS^-(Br^-)$]. The average g value is slightly smaller in the matrix than in the solid state. The $A_\parallel$ value from the well-resolved hyperfine splitting in the $g_\parallel$ signal of Cu(terpy)$(NCS)_2$ (-172×10^{-4} cm^{-1}) is significantly larger than the one in the orthorhombic g_y signal of Cu^{2+}-doped Zn(terpy)$(NCS)_2$ (-147×10^{-4} cm^{-1}; Figure 6). The derived mixing coefficient α of the $d_{x^2-y^2}$ orbital in the ground-state MO yields 0.87, in good agreement with the coefficient for Cu(II)–nitro complexes.[20] $A_\parallel$ ($=-178$ cm^{-1}) is slightly larger for the bromide. The solution and solid solution ligand field spectra exhibit a band at 14 900 cm^{-1} with a weak shoulder around 12 000 cm^{-1}, at about 10% higher energy than in case of the SP geometry. Apparently the energy, which determines the conformational change in going from the solid state to matrix isolation, is only very small. Alternatively the square-pyramidal geometry in solid solution may have been stabilized by a very weakly bonded solvent molecule in the free axial position.

(18) Vlasse, M.; Rojo, T.; Beltran-Porter, D. *Acta Crystallogr., Sect. C: Cryst. Struct. Commun.* **1983**, *C39*, 560.
(19) Einstein, F. W. B.; Penfold, B. R. *Acta Crystallogr.* **1966**, *20*, 924.
(20) Ozarowski, A.; Reinen, D. *Inorg. Chem.* **1985**, *24*, 3860.

Conclusions

The singular molecular geometries of the five-coordinate Cu(terpy)X_2 complexes with X = NCS^- and Br^- (Figure 2) can be rationalized by following a pathway that classifies the ligand displacements corresponding to the three ϵ' vibrations in D_{3h} symmetry (Figures 1 and 4).[3] The $(A_1' + E') \otimes \epsilon'$ vibronic coupling calculations for the $CuCl_5^{3-}$ model complex yield a ground-state potential surface that possesses minima for three equivalent C_{2v} geometries (nearly C_{4v} elongated square pyramids; see Figure 1) and three saddle points also with C_{2v} symmetry in the "reverse" directions (between the C_{4v} minima in Figure 1). The energy differences between the elongated square pyramid, the "reverse" geometry, and the compressed trigonal bipyramid are usually small and may even fall into the range of thermal energies.[3] It is hence apparently possible to stabilize any coordination along the ϵ' pathways with C_{2v} or even lower symmetries if steric ligand strains, the presence of different ligands, packing effects in the unit cell, or weak solvent effects are additionally present. For the two complexes under discussion, the specific geometry of the rigid terpyridine ligand seems to have been deciding for the stabilization of a geometry along the displacement coordinate in the "reverse" direction. There is no convincing evidence, either from EPR spectroscopy or from anomalous temperature ellipsoids of Cu^{2+} and the nitrogen and bromide ligator atoms, that the observed molecular geometries are dynamically averaged square-pyramidal conformations.

Acknowledgment. This work was supported in part by Grant 2930/83 from the CAICYT and by the "Deutsche Forschungsgemeinschaft", which we gratefully acknowledge.

Registry No. [Cu(terpy)Br_2], 25971-38-4; [Cu(terpy)$(NCS)_2$], 25970-65-4; [Zn(terpy)$(NCS)_2$], 115560-02-6.

Supplementary Material Available: Table S1 (anisotropic thermal parameters) and Table S2 (hydrogen coordinates and the C–H distances) (2 pages); Table S3 (calculated and observed structure factors) (9 pages). Ordering information is given on any current masthead page.

Contribution from the Departments of Chemistry, Tokyo Institute of Technology, O-okayama, Meguro-ku, Tokyo 152, Japan, and Ochanomizu University, Otsuka, Bunkyo-ku, Tokyo 112, Japan

Crystal Structure and Absolute Configuration of $(+)_{275}^{CD}$-Tris(2,4-pentanedionato)ruthenium(III)

Hideyo Matsuzawa,† Yuji Ohashi,‡ Youkoh Kaizu,† and Hiroshi Kobayashi*,†

Received February 9, 1988

The crystal structure and absolute configuration of $(+)_{275}^{CD}$-tris(2,4-pentanedionato)ruthenium(III) ($(+)_{275}^{CD}$-[Ru(acac)$_3$]) have been determined from the single-crystal X-ray data. The red crystals of $(+)_{275}^{CD}$-[Ru(acac)$_3$] obtained by condensation of the first fraction eluted by hexane/propanol from a high-performance liquid chromatography (HPLC) column of porous silica gel coated with cellulose tris(phenylcarbamate) are monoclinic with unit-cell dimensions $a = 12.750$ (3) Å, $b = 12.540$ (2) Å, $c = 11.435$ (3) Å, $\beta = 101.17$ (3)°, $V = 1793.7$ Å^3, space group $P2_1$, and $Z = 4$. The structure was solved by direct methods and refined to $R = 0.046$. $(+)_{275}^{CD}$-[Ru(acac)$_3$] has a Δ configuration of D_3 symmetry with a very slight axial elongation.

Introduction

In a previous work, we achieved a complete resolution of the enantiomeric isomers of [Ru(acac)$_3$] (acac = 2,4-pentanedionate) by high-performance liquid chromatography (HPLC) on a column of porous silica gel coated with cellulose tris(phenylcarbamate). The antipodes in the first and the second fractions ($(+)_{275}^{CD}$- and $(-)_{275}^{CD}$-[Ru(acac)$_3$]) eluted by hexane/propanol were assigned the configurations Δ and Λ, respectively.[1] Our assignment was based on the theoretically predicted circular dichroism (CD) in the intense ligand (π,π^*) exciton band at around 36×10^3 cm^{-1}. The assignment is supported by the observed CD sign of partly resolved [Ru(acac)$_3$] with the Δ isomer in excess[2] and also by those observed for completely resolved Δ-trans, Δ-cis and Λ-trans, Λ-cis diastereomers of [Ru{(+)-atc}$_3$] ((+)-atc = (+)-3-acetyl camphorate), respectively.[3]

The CD spectrum of [Ru(acac)$_3$] shows an extremum in the lowest ligand (π,π^*) band in contrast with the well-resolved dispersions observed in the ligand band of the corresponding enantiomeric isomers of chromium(III), cobalt(III), and rhodium(III) analogues.[2a] The same phenomenon was observed with

† Tokyo Institute of Technology.
‡ Ochanomizu University.

(1) Kobayashi, H.; Matsuzawa, H.; Kaizu, Y.; Ichida, A. *Inorg. Chem.* **1987**, *26*, 4318.
(2) (a) Mason, S. F.; Peacock, R. D.; Prosperi, T. *J. Chem. Soc., Dalton, Trans.* **1977**, 702. (b) Drake, A. F.; Gould, J. M.; Mason, S. F.; Rosini, C.; Woodley, F. J. *Polyhedron* **1983**, *2*, 537.
(3) Everett, G. W., Jr.; King, R. M. *Inorg. Chem.* **1972**, *11*, 2041.

0020-1669/88/1327-2981$01.50/0

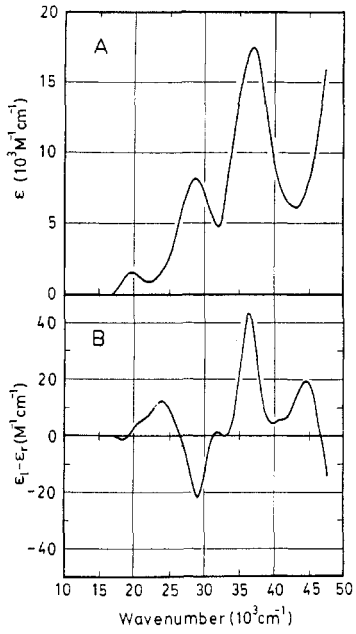

Figure 1. Absorption (A) and CD spectra (B) of $(+)^{CD}_{275}$-[Ru(acac)$_3$] in methanol. The diastereomer was isolated from the first fraction eluted by hexane/2-propanol (9:1) from a HPLC column of porous silica gel coated with cellulose tris(phenylcarbamate).

the diastereomers of [Ru{(+)-atc}$_3$].[3-5] The absolute configuration of Λ-*trans*-[Cr{(+)-atc}$_3$] was confirmed by a single-crystal X-ray study.[6]

The Λ configuration of $(-)_{546}$-[Co(acac)$_3$] was determined with quasi-racemic monoclinic crystals obtained by crystallization of a mixture of partly resolved [Co(acac)$_3$] and racemic [Al(acac)$_3$].[7] The Δ configuration of $(-)_{589}$-[Cr(acac)$_3$] was also confirmed by an X-ray study.[8] The CD spectrum in the lowest ligand (π,π^*) transition of a complex of Δ configuration such as Δ-[Si(acac)$_3$]$^+$,[9] which has no low-lying MLCT and/or LMCT excited states, is observed with Δ-[Cr(acac)$_3$] and less clearly with Δ-[Co(acac)$_3$]. However, the CD sign is not observed with Δ-[Ru(acac)$_3$].

In the present work, we determined the crystal structure and confirmed the Δ configuration of the enantiomeric isomer obtained from the early eluted fraction, $(+)^{CD}_{275}$-[Ru(acac)$_3$].

Experimental Section

Preparation and Resolution of the Enantiomeric Isomers. [Ru(acac)$_3$] was synthesized by the literature method[10] with some modification.[11] The complex was purified by chromatography on alumina (Merck alumina 90) columns with benzene as eluent, followed by recrystallization from methanol and then sublimation. A complete resolution of the enantiomeric isomers of [Ru(acac)$_3$] was achieved on a column of porous silica gel coated with cellulose tris(phenylcarbamate) (Daicel CHIRALCEL OC). A solution of 9 mg of [Ru(acac)$_3$] dissolved in 2 mL of a 7:1 mixed solvent of ethanol and hexane/2-propanol (9:1) was loaded onto the column and then eluted by a hexane/2-propanol (9:1) mixture: $\Delta\epsilon = \epsilon_L - \epsilon_R = 43.6$ M^{-1} cm^{-1} at 275 nm.

The enantiomers were separated on a semipreparative scale by using a CHIRALCEL OC column (0.46 cm i.d. × 25 cm length). The enantiomeric excess of the first fraction of elution was 100% while that of the second was 91%, respectively. However, another run with the second fraction yields complete resolution. From the elutions, the antipodes were obtained by evaporation of solvent under reduced pressure in a water bath at 30 °C.

HPLC resolution on the stationary chiral phase packed column was carried out at 22 °C and a flow rate of 1.0 mL/min by use of a JASCO BIP-I HPLC pump with a Uvidec-100V variable-wavelength detector. The optical purity was measured with the UV detector operated at 270 nm.

Figure 1 shows absorption and CD spectra of a methanol solution of the enantiomeric isomer obtained from the first fraction of elution, $(+)^{CD}_{275}$-[Ru(acac)$_3$]. The absorption spectrum was recorded on a Hitachi 330 spectrophotometer, and the CD spectrum was taken on a JASCO J-500C spectropolarimeter.

Structure Determination. The red single crystals of $(+)^{CD}_{275}$-[Ru(acac)$_3$] were grown from a methanol solution in a glass tube placed in a water bath. The symmetry and approximate cell dimensions of the crystal were determined from oscillation and Weissenberg photographs. The most accurate cell dimensions were obtained by the least-squares analysis of 2θ values measured on a Rigaku AFC automated four-circle diffractometer. The crystal data of $(+)^{CD}_{275}$-[Ru(acac)$_3$] are summarized in Table I.

Intensity data up to $2\theta \leq 55°$ were collected at room temperature with use of a crystal of size 0.3 × 0.25 × 0.2 mm on the diffractometer using graphite-monochromated Mo Kα radiation (λ = 0.71069 Å). An ω–2θ scan was employed with a scan rate (in 2θ) of 8° min^{-1}. Stationary background counts were accumulated for 5 s before and after each scan. A total of 4027 independent reflections ($|F_o| \geq 3\sigma(|F_o|)$) were used for the structure determination. The intensities were corrected for Lorentz and polarization factors, but the absorption correction was not applied.

The structure was solved by direct methods using MULTAN 78[12] and refined by a constrained least-squares method using the SHELX 76 program[13] in order to avoid parameter interaction between the two crystallographically independent molecules present in the asymmetric unit of space group $P2_1$. The non-hydrogen atoms were refined anisotropically by using F_o module weighted according to $\omega = \{\sigma(|F_o|)^2 + 0.00400F_o^2\}^{-1}$. After the refinement converged, the hydrogen atoms were introduced in constraint with the fixed C–H distance of 1.10 Å and the fixed isotropic temperature factor $B = 10.0$ Å^2. A further refinement was carried out by a block-diagonal least-squares method using a modified HBLS program.[14] The weighting scheme of $\omega = \{\sigma(|F_o|)^2 + 0.0025F_o^2\}^{-1}$ was employed. The positional parameters, including those of hydrogen atoms,

Table I. Crystal Data for $(+)^{CD}_{275}$-[Ru(acac)$_3$]

formula	$Ru(C_5H_7O_2)_3$	β, deg	101.17 (3)
fw	398.38	V, Å^3	1793.7
space group	$P2_1$	Z	4
a, Å	12.750 (3)	d_{calcd}, g/cm^3	1.476
b, Å	12.540 (2)	μ(Mo Kα), cm^{-1}	8.78
c, Å	11.435 (3)	F(000)	812

Table II. Determination of the Absolute Configuration: Relations of $|F|$ in Friedel Pairs for the Δ Configuration

hkl	$\lvert F_c(hkl)\rvert$	obsd rel	$\lvert F_c(\bar{h}\bar{k}\bar{l})\rvert$
160	484	>	428
180	160	>	109
490	174	<	207
$\bar{4}11$	447	>	400
051	399	>	353
251	183	<	213
$\bar{3}12$	350	>	306
212	228	<	269
143	311	>	251
085	108	>	76
$\bar{4}63$	267	>	231
$\bar{2}63$	210	>	180
163	366	>	317
$\bar{4}27$	288	>	250
037	154	<	184
$\bar{1}57$	199	>	158
058	289	>	243
$\bar{7}28$	230	<	264
414	313	<	376
$\bar{6}24$	406	<	448

(4) King, R. M.; Everett, G. W., Jr. *Inorg. Chem.* **1971**, *10*, 1237.
(5) Everett, G. W., Jr.; Johnson, A. *Inorg. Chem.* **1974**, *13*, 489.
(6) Horrocks, W. D., Jr.; Johnston, D. L.; MacInnes, D. *J. Am. Chem. Soc.* **1970**, *92*, 7620.
(7) Von Dreele, R. B.; Fay, R. C. *J. Am. Chem. Soc.* **1971**, *93*, 4936.
(8) Kuroda, R.; Mason, S. F. *J. Chem. Soc., Dalton Trans.* **1979**, 273.
(9) Larsen, E.; Mason, S. F.; Searle, G. H. *Acta Chem. Scand.* **1966**, *20*, 191.
(10) Wilkinson, G. *J. Am. Chem. Soc.* **1952**, *74*, 6146.
(11) Endo, A.; Shimizu, K.; Sato, G. P.; Mukaida, M. *Chem. Lett.* **1984**, 437.
(12) Main, P.; Lessinger, L.; Woolfson, M. M.; Germain, G.; Declercq, J. P. "MULTAN 78, A System of Computer Programs for the Automatic Solution of Crystal Structure from X-ray Diffraction Data"; University of York, York, England, and University of Louvain, Louvain, Belgium, 1978.
(13) Sheldrick, G. M. "SHELX-76, Program for Crystal Structure Determinations"; University of Cambridge, Cambridge, England, 1976.
(14) Ohashi, Y., unpublished version (1975) of a program originally written by T. Ashida.

Table III. Final Atomic Coordinates and Thermal Parameters with Estimated Standard Deviations in Parentheses

atom	x, a	y, b	z, c	B or B_{eq},[a] Å^2	atom	x, a	y, b	z, c	B or B_{eq},[a] Å^2
Ru(1)	0.90395 (5)	0.62933[b]	0.63109 (5)	3.98 (2)	C(7F)	0.0565 (8)	0.5452 (11)	0.0162 (9)	6.5 (3)
O(1A)	0.8801 (5)	0.6706 (5)	0.7925 (5)	5.0 (2)	H(3A)	0.755 (9)	0.863 (12)	0.777 (10)	10 (4)
O(5A)	0.8172 (4)	0.7531 (5)	0.5510 (4)	4.2 (1)	H(3B)	0.829 (7)	0.315 (9)	0.703 (7)	7 (2)
O(1B)	0.9960 (5)	0.5072 (6)	0.7044 (5)	6.0 (2)	H(3C)	1.179 (6)	0.640 (8)	0.488 (7)	5 (2)
O(5B)	0.7674 (5)	0.5472 (5)	0.6073 (5)	4.7 (2)	H(6A1)	0.711 (10)	0.843 (13)	0.933 (10)	11 (4)
O(1C)	1.0373 (5)	0.7193 (6)	0.6589 (5)	5.7 (2)	H(6A2)	0.875 (7)	0.756 (9)	0.980 (8)	7 (2)
O(5C)	0.9299 (5)	0.5788 (6)	0.4740 (4)	5.3 (2)	H(6A3)	0.788 (9)	0.707 (11)	0.981 (9)	10 (3)
C(2A)	0.8153 (7)	0.7441 (7)	0.8096 (7)	4.5 (2)	H(7A1)	0.683 (10)	0.963 (13)	0.587 (10)	11 (4)
C(4A)	0.7630 (6)	0.8159 (6)	0.6061 (7)	4.1 (2)	H(7A2)	0.644 (6)	0.856 (7)	0.480 (6)	4 (2)
C(2B)	0.9552 (12)	0.4138 (10)	0.7110 (9)	7.7 (4)	H(7A3)	0.761 (7)	0.940 (8)	0.495 (7)	5 (2)
C(4B)	0.7602 (9)	0.4493 (9)	0.6374 (8)	6.4 (3)	H(6B1)	1.004 (8)	0.264 (9)	0.749 (8)	7 (3)
C(2C)	1.1099 (7)	0.7083 (11)	0.5980 (8)	6.2 (3)	H(6B2)	1.077 (9)	0.351 (12)	0.808 (10)	11 (4)
C(4C)	1.0217 (7)	0.5863 (8)	0.4433 (6)	4.9 (2)	H(6B3)	1.076 (10)	0.290 (12)	0.692 (10)	14 (4)
C(3A)	0.7632 (7)	0.8130 (7)	0.7290 (8)	5.1 (3)	H(7B1)	0.651 (7)	0.333 (9)	0.661 (7)	6 (2)
C(3B)	0.8491 (11)	0.3844 (9)	0.6857 (10)	7.5 (4)	H(7B2)	0.616 (8)	0.414 (8)	0.544 (8)	7 (3)
C(3C)	1.1055 (8)	0.6420 (10)	0.5009 (9)	6.7 (3)	H(7B3)	0.619 (9)	0.452 (11)	0.675 (9)	9 (3)
C(6A)	0.8040 (10)	0.7561 (12)	0.9372 (8)	8.0 (4)	H(6C1)	1.238 (9)	0.776 (13)	0.589 (10)	13 (4)
C(7A)	0.7009 (9)	0.9001 (8)	0.5287 (11)	6.4 (3)	H(6C2)	1.232 (9)	0.761 (11)	0.719 (10)	12 (4)
C(6B)	1.0356 (14)	0.3270 (13)	0.7517 (13)	11.1 (6)	H(6C3)	1.190 (10)	0.833 (12)	0.634 (10)	13 (4)
C(7B)	0.6537 (11)	0.4060 (11)	0.6251 (12)	8.2 (5)	H(7C1)	1.115 (7)	0.528 (8)	0.320 (7)	6 (2)
C(6C)	1.2069 (10)	0.7769 (17)	0.6445 (14)	11.5 (7)	H(7C2)	0.977 (8)	0.581 (9)	0.271 (8)	7 (3)
C(7C)	1.0273 (11)	0.5225 (11)	0.3294 (10)	8.0 (4)	H(7C3)	1.002 (12)	0.461 (15)	0.346 (11)	14 (5)
Ru(2)	0.38655 (4)	0.61044 (6)	0.13918 (4)	2.85 (1)	H(3D)	0.649 (5)	0.626 (6)	0.421 (5)	3 (1)
O(1D)	0.5383 (4)	0.6538 (5)	0.1492 (4)	3.9 (1)	H(3E)	0.451 (6)	0.354 (7)	−0.058 (6)	4 (2)
O(5D)	0.3928 (4)	0.6375 (4)	0.3145 (4)	3.6 (1)	H(3F)	0.097 (9)	0.734 (11)	−0.059 (10)	11 (4)
O(1E)	0.3787 (4)	0.5869 (4)	−0.0349 (4)	3.5 (1)	H(6D1)	0.767 (8)	0.643 (10)	0.303 (9)	9 (3)
O(5E)	0.4380 (4)	0.4638 (4)	0.1861 (4)	3.4 (1)	H(6D2)	0.732 (8)	0.709 (10)	0.176 (9)	9 (3)
O(1F)	0.3353 (5)	0.7608 (5)	0.0958 (5)	4.5 (2)	H(6D3)	0.704 (10)	0.629 (13)	0.196 (11)	12 (4)
O(5F)	0.2362 (4)	0.5599 (4)	0.1188 (4)	3.8 (1)	H(7D1)	0.531 (6)	0.648 (8)	0.554 (6)	6 (2)
C(2D)	0.6071 (6)	0.6506 (8)	0.2493 (7)	4.3 (2)	H(7D2)	0.408 (5)	0.610 (6)	0.532 (6)	3 (1)
C(4D)	0.4830 (7)	0.6405 (6)	0.3898 (6)	4.1 (2)	H(7D3)	0.484 (10)	0.725 (11)	0.547 (9)	10 (3)
C(2E)	0.4064 (7)	0.4989 (8)	−0.0761 (6)	4.6 (2)	H(6E1)	0.382 (10)	0.439 (12)	−0.244 (10)	11 (4)
C(4E)	0.4621 (6)	0.3948 (7)	0.1121 (7)	4.2 (2)	H(6E2)	0.420 (10)	0.516 (13)	−0.259 (11)	12 (4)
C(2F)	0.2460 (8)	0.7832 (8)	0.0393 (8)	5.4 (3)	H(6E3)	0.300 (10)	0.508 (12)	−0.227 (11)	12 (4)
C(4F)	0.1586 (5)	0.6086 (9)	0.0482 (6)	4.4 (2)	H(7E1)	0.525 (8)	0.256 (10)	0.107 (8)	8 (3)
C(3D)	0.5823 (6)	0.6441 (8)	0.3607 (6)	4.2 (2)	H(7E2)	0.452 (6)	0.269 (7)	0.201 (6)	4 (2)
C(3E)	0.4452 (8)	0.4111 (7)	−0.0138 (8)	5.1 (3)	H(7E3)	0.574 (9)	0.291 (11)	0.232 (10)	11 (4)
C(3F)	0.1605 (7)	0.7137 (9)	0.0090 (9)	6.0 (3)	H(6F1)	0.184 (10)	0.924 (12)	−0.063 (10)	13 (4)
C(6D)	0.7227 (7)	0.6625 (13)	0.2371 (9)	7.5 (4)	H(6F2)	0.342 (10)	0.929 (12)	0.010 (10)	10 (4)
C(7D)	0.4706 (8)	0.6501 (10)	0.5188 (7)	6.0 (3)	H(6F3)	0.233 (10)	0.942 (14)	0.067 (10)	13 (4)
C(6E)	0.3882 (12)	0.4997 (12)	−0.2124 (8)	8.4 (5)	H(7F1)	0.008 (11)	0.580 (13)	−0.033 (10)	11 (4)
C(7E)	0.5037 (9)	0.2909 (9)	0.1604 (9)	6.5 (3)	H(7F2)	0.036 (11)	0.535 (14)	0.069 (10)	14 (5)
C(6F)	0.2304 (11)	0.8973 (9)	−0.0033 (11)	8.4 (4)	H(7F3)	0.061 (10)	0.493 (13)	−0.021 (11)	13 (5)

[a] B_{eq} means the equivalent isotropic thermal parameter for non-hydrogen atoms, defined by $B_{eq} = {}^4/_3[a^2\beta(1,1) + b^2\beta(2,2) + c^2\beta(3,3) + ab(\cos\gamma)\beta(1,2) + ac(\cos\beta)\beta(1,3) + bc(\cos\alpha)\beta(2,3)]$.[17] [b] Ru(1) y value was fixed in accord with the space group requirement.

were refined up to an R value of 0.046 and $R_w = 0.066$ (R_w being defined by $\{w\sum(|F_o| - |F_c|)^2/w\sum|F_o|^2\}^{1/2}$). No peaks higher than 0.52 e Å^{-3} were found on the difference map. The atomic scattering factors including the anomalous terms of Mo Kα radiation were taken from ref 15.

The computation was carried out on a HITAC system M-680H computer at the University of Tokyo Computer Center.

Results and Discussion

Absolute Configuration. The intensities of 20 Friedel pairs (hkl and $\bar{h}\bar{k}\bar{l}$) for which differences in intensities were the largest were measured on the diffractometer using graphite-monochromated Cu Kα radiation. The structure factors were calculated for the Δ configuration by use of the values of anomalous scattering terms of ruthenium given in the literature.[15] All the relations between $|F_c(hkl)|$ and $|F_c(\bar{h}\bar{k}\bar{l})|$ are consistent with those between $|F_o(hkl)|$ and $|F_o(\bar{h}\bar{k}\bar{l})|$, indicating that $(+)^{CD}_{275}$-[Ru(acac)$_3$] is in the Δ configuration. Table II presents the relations between $|F_c(hkl)|$ and $|F_c(\bar{h}\bar{k}\bar{l})|$ and the corresponding $|F_o(hkl)|$ and $|F_o(\bar{h}\bar{k}\bar{l})|$.

Structure of [Ru(acac)$_3$]. The crystal structure of Δ-[Ru(acac)$_3$] viewed along the b axis is shown in Figure 2. Table III summarizes the final atomic coordinates.

As Figure 2 shows, the two crystallographically independent complexes (referred to as I and II) are related by a pseudo inversion center in the unit cell. The complexes I and II (containing Ru(1) and Ru(2), respectively) are of identical configuration. Their structures are not significantly different from each other, and the corresponding intramolecular bond distances and bond angles, which are given in Table IV, are very similar. The ligand skeletal atoms are designated with the numbers 1–7 for each ligand (A–C on Ru(1) and D–F on Ru(2)), while the peripheral hydrogens are designated with the numbering of the attached carbon atoms.

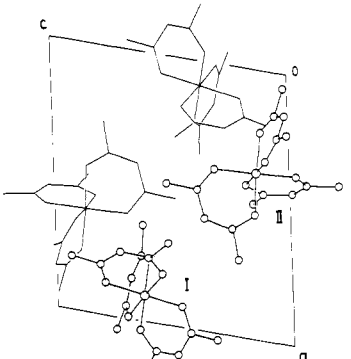

Figure 2. Projection of the Δ-[Ru(acac)$_3$] crystal structure on the ac plane viewed down the b axis. The heavier and lighter lines refer to molecules separated along the b axis by $y = {}^1/_2$.

(15) Ibers, J. A.; Hamilton, W. C. *International Tables for X-ray Crystallography*; Kynoch: Birmingham, England, 1974; Vol. IV, pp 72–150.

Table IV. Bond Distances (Å) and Bond Angles (deg) in the Coordination Sphere of Δ-[Ru(acac)$_3$]

molecule I		molecule II		molecule I		molecule II	
			Distances				
Ru(1)–O(1A)	1.996 (6)	Ru(2)–O(1D)	1.991 (5)	C(2A)–C(3A)	1.341 (12)	C(2D)–C(3D)	1.372 (11)
Ru(1)–O(5A)	2.019 (5)	Ru(2)–O(5D)	2.019 (5)	C(4A)–C(3A)	1.405 (13)	C(4D)–C(3D)	1.371 (12)
Ru(1)–O(1B)	2.011 (7)	Ru(2)–O(1E)	1.995 (4)	C(2B)–C(3B)	1.379 (20)	C(2E)–C(3E)	1.352 (13)
Ru(1)–O(5B)	1.995 (6)	Ru(2)–O(5E)	1.990 (5)	C(4B)–C(3B)	1.417 (17)	C(4E)–C(3E)	1.428 (12)
Ru(1)–O(1C)	2.013 (7)	Ru(2)–O(1F)	2.025 (6)	C(2C)–C(3C)	1.379 (16)	C(2F)–C(3F)	1.386 (14)
Ru(1)–O(5C)	1.992 (6)	Ru(2)–O(5F)	1.990 (5)	C(4C)–C(3C)	1.338 (13)	C(4F)–C(3F)	1.394 (16)
av	2.004 (6)	av	2.002 (5)	av	1.377 (15)	av	1.384 (13)
O(1A)–C(2A)	1.278 (11)	O(1D)–C(2D)	1.301 (8)	C(2A)–C(6A)	1.502 (13)	C(2D)–C(6D)	1.515 (13)
O(5A)–C(4A)	1.290 (10)	O(5D)–C(4D)	1.297 (8)	C(4A)–C(7A)	1.501 (13)	C(4D)–C(7D)	1.518 (11)
O(1B)–C(2B)	1.290 (15)	O(1E)–C(2E)	1.277 (11)	C(2B)–C(6B)	1.505 (21)	C(2E)–C(6E)	1.531 (12)
O(5B)–C(4B)	1.283 (13)	O(5E)–C(4E)	1.288 (10)	C(4B)–C(7B)	1.444 (19)	C(4E)–C(7E)	1.473 (14)
O(1C)–C(2C)	1.269 (12)	O(1F)–C(2F)	1.228 (11)	C(2C)–C(6C)	1.516 (19)	C(2F)–C(6F)	1.513 (15)
O(5C)–C(4C)	1.289 (11)	O(5F)–C(4F)	1.301 (9)	C(4C)–C(7C)	1.542 (15)	C(4F)–C(7F)	1.509 (14)
av	1.283 (12)	av	1.282 (9)	av	1.502 (17)	av	1.510 (13)
			Angles				
O(1A)–Ru(1)–O(5A)[a]	93.0 (2)	O(1D)–Ru(2)–O(5D)[a]	92.6 (2)	C(2A)–C(3A)–C(4A)	127.5 (1.2)	C(2D)–C(3D)–C(4D)	128.0 (1.1)
O(1B)–Ru(1)–O(5B)[a]	95.0 (3)	O(1E)–Ru(2)–O(5E)[a]	94.7 (2)	C(2B)–C(3B)–C(4B)	127.4 (1.8)	C(2E)–C(3E)–C(4E)	128.0 (1.2)
O(1C)–Ru(1)–O(5C)[a]	92.2 (3)	O(1F)–Ru(2)–O(5F)[a]	90.6 (2)	C(2C)–C(3C)–C(4C)	128.0 (1.5)	C(2F)–C(3F)–C(4F)	125.2 (1.3)
av	93.4 (3)	av	92.6 (2)	av	127.6 (1.5)	av	127.1 (1.2)
Ru(1)–O(1A)–C(2A)	123.2 (7)	Ru(2)–O(1D)–C(2D)	121.6 (6)	O(1A)–C(2A)–C(6A)	114.1 (1.1)	O(1D)–C(2D)–C(6D)	114.7 (9)
Ru(1)–O(5A)–C(4A)	123.0 (6)	Ru(2)–O(5D)–C(4D)	121.6 (5)	O(5A)–C(4A)–C(7A)	114.3 (1.0)	O(5D)–C(4D)–C(7D)	113.7 (8)
Ru(1)–O(1B)–C(2B)	120.4 (9)	Ru(2)–O(1E)–C(2E)	122.2 (6)	O(1B)–C(2B)–C(6B)	114.6 (1.5)	O(1E)–C(2E)–C(6E)	111.8 (1.0)
Ru(1)–O(5B)–C(4B)	124.3 (8)	Ru(2)–O(5E)–C(4E)	123.5 (6)	O(5B)–C(4B)–(C7B)	116.7 (1.3)	O(5E)–C(4E)–C(7E)	117.6 (1.1)
Ru(1)–O(1C)–C(2C)	122.4 (8)	Ru(2)–O(1F)–C(2F)	124.3 (7)	O(1C)–C(2C)–C(6C)	112.2 (1.3)	O(1F)–C(2F)–C(6F)	115.9 (1.1)
Ru(1)–O(5C)–C(4C)	122.7 (7)	Ru(2)–O(5F)–C(4F)	121.5 (5)	O(5C)–C(4C)–C(7C)	112.7 (1.1)	O(5F)–C(4F)–C(7F)	114.9 (1.0)
av	122.7 (7)	av	122.4 (6)	av	114.1 (1.2)	av	114.8 (1.0)
O(1A)–C(2A)–C(3A)	127.4 (1.2)	O(1D)–C(2D)–C(3D)	125.6 (9)	C(3A)–C(2A)–C(6A)	118.4 (1.1)	C(3D)–C(2D)–C(6D)	119.6 (1.0)
O(5A)–C(4A)–C(3A)	125.1 (1.1)	O(5D)–C(4D)–C(3D)	125.6 (9)	C(3A)–C(4A)–C(7A)	120.5 (1.2)	C(3D)–C(4D)–C(7D)	120.5 (1.0)
O(1B)–C(2B)–C(3B)	128.4 (1.7)	O(1E)–C(2E)–C(3E)	127.5 (1.1)	C(3B)–C(2B)–C(6B)	117.0 (1.6)	C(3E)–C(2E)–C(6E)	120.6 (1.2)
O(5B)–C(4B)–C(3B)	124.1 (1.4)	O(5E)–C(4E)–C(3E)	123.9 (1.0)	C(3B)–C(4B)–C(7B)	119.2 (1.5)	C(3E)–C(4E)–C(7E)	118.5 (1.1)
O(1C)–C(2C)–C(3C)	125.9 (1.4)	O(1F)–C(2F)–C(3F)	126.3 (1.2)	C(3C)–C(2C)–C(6C)	121.9 (1.7)	C(3F)–C(2F)–C(6F)	117.8 (1.2)
O(5C)–C(4C)–C(3C)	125.8 (1.2)	O(5F)–C(4F)–C(3F)	125.7 (1.2)	C(3C)–C(4C)–C(7C)	121.6 (1.3)	C(3F)–C(4F)–C(7F)	119.2 (1.3)
av	126.1 (1.3)	av	125.8 (1.1)	av	119.7 (1.4)	av	119.4 (1.1)

[a] "Bite" angle.

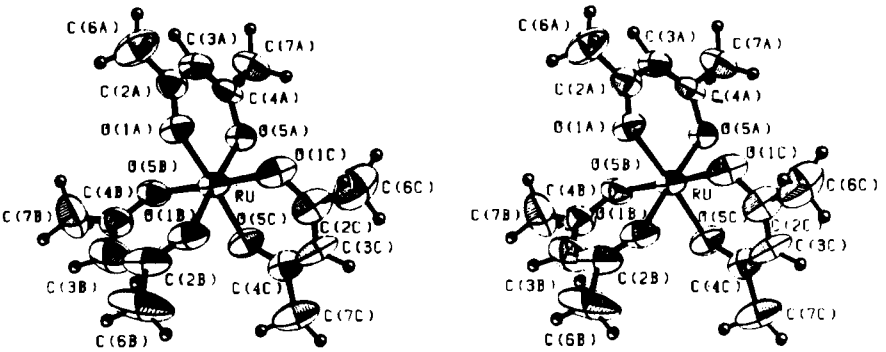

Figure 3. Stereoview of Δ-[Ru(acac)$_3$]. Thermal ellipsoids are drawn at the 50% probability level. H atoms are represented by spheres of arbitrary size.

Figure 3 presents a stereoview[16] of Δ-[Ru(acac)$_3$] with species I. Both complexes I and II are approximately of D_3 symmetry but form an almost regular octahedron of RuO_6. The average Ru–O distance and O–Ru–O "bite angle" are 2.003 Å and 93.0°, respectively.

The polar angles (θ) of Ru–O bonds with respect to the 3-fold axis of D_3 symmetry are at an average value of 54.0° in each of the complexes I and II as compared with θ = 54.74° for a regular octahedron, while the mean value of azimuthal projection (ϕ) of the intrachelate O–Ru–O (bite) angles (93.0°) is 64.0° in contrast with ϕ = 60° for the octahedron.

An octahedron is viewed as a D_{3d} trigonal prism with the two parallel staggered equilateral triangles of side s at a distance of h.[18] The ratio $s/h = 3^{1/2} \tan \theta/2 = 1.19$ for Δ-[Ru(acac)$_3$] as compared with the value $s/h = (^3/_2)^{1/2} = 1.22$ of the regular octahedron indicates a slight elongation of the RuO_6 coordination octahedron along the direction of the 3-fold axis. The molecular structure determined with Δ-[Ru(acac)$_3$] in the present work is qualitatively reproduced in that of the racemic mixture: Δ-[Ru(acac)$_3$], Ru–O = 2.003 (6) Å, O–Ru–O = 93.0 (3)°, O–O bite distance = 2.906 (8) Å, ϕ = 64.0°, θ = 54.0°; *rac*-[Ru(acac)$_3$], Ru–O = 1.99 (2) Å, O–Ru–O = 93.7 (9)°, O–O bite distance = 2.91 (3) Å, ϕ = 64.4°, θ = 53.9°.[19] So far the molecular structures of the tervalent-metal analogues, including [Al(acac)$_3$],[20] [Cr(acac)$_3$],[21] [Mn(acac)$_3$],[22] [Co(acac)$_3$],[20,23] [Ga(acac)$_3$],[24] and

(16) Johnston, C. K. "ORTEP Thermal-Ellipsoid Plot Program for Crystal Structure Illustrations"; Report No. ORNL-3794, Oak Ridge National Laboratory, Oak Ridge, TN, 1965.
(17) Willis, B. T. M.; Pryor, A. W. *Thermal Vibrations in Crystallography*; Cambridge University Press: London, 1975; p 101.
(18) Stiefel, E. I.; Brown, G. F. *Inorg. Chem.* **1972**, *11*, 434.
(19) Chao, G. K.-J.; Sime, R. L.; Sime, R. J. *Acta Crystallogr., Sect. B: Struct. Crystallogr. Cryst. Chem.* **1973**, *B29*, 2845.
(20) Hon, P. K.; Pfluger, C. E. *J. Coord. Chem.* **1973**, *3*, 67.
(21) Morosin, B. *Acta Crystallogr.* **1965**, *19*, 131.
(22) Fackler, J. P., Jr.; Avdeef, A. *Inorg. Chem.* **1974**, *13*, 1864.
(23) Kruger, G. J.; Reynhardt, E. C. *Acta Crystallogr., Sect. B: Struct. Crystallogr. Cryst. Chem.* **1974**, *B30*, 822.

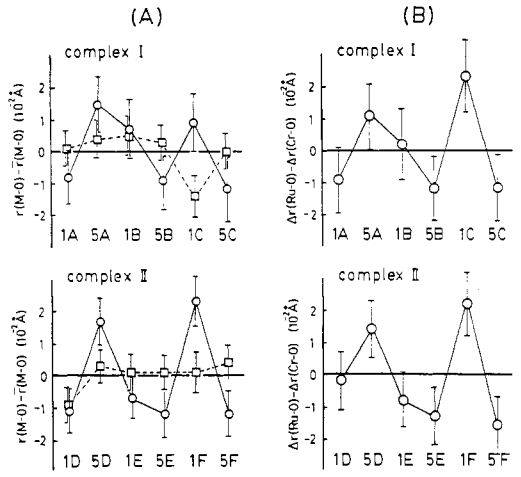

Figure 4. (A) Plots of the variations of M–O bond distances from the respective average values (r(M–O) – $\bar{r}$(M–O) = Δr(M–O)) in Δ-[Ru(acac)$_3$] (—) and Δ-[Cr(acac)$_3$] (- - -, taken from ref 8). (B) Plots of the differences of the corresponding Ru–O and Cr–O bond distances (Δr(Ru–O) – Δr(Cr–O)).

[Rh(acac)$_3$],[25] have been determined with their racemic mixtures in isomorphous crystals ($P2_1/c$). An increase of the size of metal ion (Al, Cr, Mn, Co, Ga, Rh) results in an increase of the O–O bite distances (2.726, 2.786, 2.791, 2.817, 2.802, and 2.946 Å, respectively). However, the ratio s/h persists at around the value for the regular octahedron. The average values of structural parameters obtained with Δ-[Ru(acac)$_3$] indicate that the RuO_6 polyhedron in [Ru(acac)$_3$] is in a regular octahedron even if the central metal ion has an open-shell d_π^5 system in contrast with the totally symmetric system of [Al(acac)$_3$], [Cr(acac)$_3$], [Co(acac)$_3$], [Ga(acac)$_3$], and [Rh(acac)$_3$].

The packing mode of Δ-[Ru(acac)$_3$] is very similar to that of Δ-[Cr(acac)$_3$] in isomorphous crystals ($P2_1$). Despite the increase in the size of the metal ion, the dimension of the unit cell is not very different: Δ-[Ru(acac)$_3$], a = 12.750 (3) Å, b = 12.540 (2) Å, c = 11.435 (3) Å, β = 101.17 (3)°; Δ-[Cr(acac)$_3$], a = 12.720 (3) Å, b = 12.643 (4) Å, c = 11.443 (3) Å, β = 101.08 (4)°.[8] The crystals of the corresponding racemic mixtures are more contracted than those of the enantiomeric isomers: Δ-[Ru(acac)$_3$], V = 1794 Å^3, d_{calcd} = 1.476 g cm^{-3}; *rac*-[Ru(acac)$_3$], V = 1650 Å^3, d_{calcd} = 1.59 g cm^{-3};[19] Δ-[Cr(acac)$_3$], V = 1806 Å^3, d_{calcd} = 1.285 g cm^{-3};[8] *rac*-[Cr(acac)$_3$], V = 1714 Å^3, d_{calcd} = 1.362 g cm^{-3}.[21] The higher density of the racemic mixtures is due to the tight packing of closely contacting pairs of Δ and Λ isomers in the unit cell. However, it should be noted that the packing in the crystals of enantiomeric isomers yields a greater variation of the M–O distances in Δ-[Ru(acac)$_3$] than in Δ-[Cr(acac)$_3$] despite their very similar dimensions of unit cell.

Figure 4A presents plots of the deviations of the M–O distances from the respective average values (Δr(M–O) = r(M–O) – $\bar{r}$(M–O)) in Δ-[Ru(acac)$_3$] and Δ-[Cr(acac)$_3$]. The variation of the Cr–O bond distances is induced predominantly by the crystal packing in Δ-[Cr(acac)$_3$]. The packing effect should yield a very analogous variation of the Ru–O bond distances in Δ-[Ru(acac)$_3$]. Thus, the variation of Δr(Ru–O) – Δr(Cr–O) is attributable to distortion such as that which originates from the Jahn–Teller effect rather than distortion due to the packing mode in the crystal. In fact, as Figure 4B shows, the plots of Δr(Ru–O) – Δr(Cr–O) are synchronous in complexes I and II.

The variation of Ru–O bond lengths is ascribed to an in-plane distortion of the regular triangle perpendicular to the 3-fold axis of [Ru(acac)$_3$]. This distortion can be described by superposition of two sets of degenerate Jahn–Teller modes, symmetric and antisymmetric S_{2a} and S_{2b} modes, which are due to the anisotropic migration of ligand π electrons into the open-shell low-spin d^5 system. The Jahn–Teller modes are given in terms of the distortion of M-O distances from regular octahedron: $S_{2a}(\mathrm{sym}) = (1/12)^{1/2}[2\Delta r_{1A} + 2\Delta r_{5A} - \Delta r_{1B} - \Delta r_{5B} - \Delta r_{1C} - \Delta r_{5C}]$, $S_{2b}(\mathrm{sym}) = 1/2[\Delta r_{1B} + \Delta r_{5B} - \Delta r_{1C} - \Delta r_{5C}]$, $S_{2a}(\mathrm{anti}) = (1/12)^{1/2}[2\Delta r_{1A} - 2\Delta r_{5A} - \Delta r_{1B} + \Delta r_{5B} - \Delta r_{1C} + \Delta r_{5C}]$, and $S_{2b}(\mathrm{anti}) = 1/2[\Delta r_{1B} - \Delta r_{5B} - \Delta r_{1C} + \Delta r_{5C}]$, where Δr_{1A} and Δr_{5A} denote the stretching of bonds Ru–O(1) and Ru–O(5) of ligand A, respectively.

In this particular d_π^5 system, however, the potential wells are not so deep that the lowest representative point of normal distortions makes a drift between the energy minima. This results in a dynamic Jahn–Teller effect. Fackler ascribed the tetragonal distortion found with [Mn(acac)$_3$] to a Jahn–Teller distortion of the high-spin d^4 system,[22] which is caused by the anisotropy of ligand σ donation to the metal $d_{x^2-y^2}$ and d_{z^2} orbitals. In the case of [Ru(acac)$_3$], however, the anisotropy is induced by ligand π donation to the open-shell metal d_π orbitals. The time-averaged geometry of [Ru(acac)$_3$] in solution must be a regular octahedron. However, the crystal packing freezes the complex in a distorted geometry that is present at one of the potential energy minima.

Highly anisotropic ESR signals (g_1 = 2.82, g_2 = 1.74, and g_3 = 1.28) were observed at 80 K with a single crystal of [Ru(acac)$_3$] diluted in isomorphous [Al(acac)$_3$],[26] while the lattice parameters and thus the packing structure were those of the host crystal. A different set of anisotropic g values ($|g_\perp|$ = 2.45, 2.16 and $|g_\parallel|$ = 1.45) were obtained with pure [Ru(acac)$_3$] and [Ru(acac)$_3$] in various glasses at 77 K.[27] The anisotropy induced perpendicular to the 3-fold axis is attributable to a Jahn–Teller distortion of the metal d_π^5 system. In fluid media at ambient temperature, the structure of the RuO_6 octahedron in [Ru(acac)$_3$] is rather dynamic and must be seen as a time-averaged regular octahedron. However, the highly anisotropic ESR signals observed in rigid matrices at 77 K, which vary with media and host crystals, can be interpreted as due to Jahn–Teller distortion, which results in a further stabilization of the complex for an increase of ligand π donation.

Acknowledgment. We thank Dr. Akito Ichida of Daicel Chemical Industries, Ltd., Tokyo, for his contribution to resolution of the optical isomers by high-performance liquid chromatography. H.M. is grateful to Dr. Akira Uchida of the Laboratory for Chemistry of Natural Products, Tokyo Institute of Technology, who instructed how to draw the ORTEP stereoview.

Registry No. Δ-[Ru(acac)$_3$], 31378-27-5.

Supplementary Material Available: Anisotropic thermal parameters for non-hydrogen atoms (Table S1) and additional bond distances and angles (Tables S2) (4 pages); observed and calculated structure factors (Table S3) (11 pages). Ordering information is given on any current masthead page.

(24) Dymock, K.; Palenik, G. J. *Acta Crystallogr., Sect. B: Struct. Crystallogr. Cryst. Chem.* **1974**, *B30*, 1364.
(25) Morrow, J. C.; Parker, E. B., Jr. *Acta Crystallogr., Sect. B: Struct. Crystallogr. Cryst. Chem.* **1973**, *B29*, 1145.
(26) Jarrett, H. S. *J. Chem. Phys.* **1957**, *27*, 1298.
(27) DeSimone, R. E. *J. Am. Chem. Soc.* **1973**, *95*, 6238.